

SCIENTIFIC REPORTS



OPEN

Tumor heterogeneity of pancreas head cancer assessed by CT texture analysis: association with survival outcomes after curative resection

Gabin Yun¹, Young Hoon Kim ¹, Yoon Jin Lee¹, Bohyoung Kim^{1,2}, Jin-Hyeok Hwang³ & Dong Joon Choi¹

The value of image based texture features as a powerful method to predict prognosis and assist clinical management in cancer patients has been established recently. However, texture analysis using histograms and grey-level co-occurrence matrix in pancreas cancer patients has rarely been reported. We aimed to analyze the association of survival outcomes with texture features in pancreas head cancer patients. Eighty-eight pancreas head cancer patients who underwent preoperative CT images followed by curative resection were included. Texture features using different filter values were obtained. The texture features of average, contrast, correlation, and standard deviation with no filter, and fine to medium filter values as well as the presence of nodal metastasis were significantly different between the recurred ($n = 70$, 79.5%) and non-recurred group ($n = 18$, 20.5%). In the multivariate Cox regression analysis, lower standard deviation and contrast and higher correlation with lower average value representing homogenous texture were significantly associated with poorer DFS (disease free survival), along with the presence of lymph node metastasis. Texture parameters from routinely performed pre-operative CT images could be used as an independent imaging tool for predicting the prognosis in pancreas head cancer patients who underwent curative resection.

With a dismal 5-year survival rate of less than 5%, ductal adenocarcinoma of the pancreas remains a lethal disease for most patients¹. While the only potentially curative treatment proven to prolong survival for pancreas cancer patients is surgical resection, only 15% to 20% of cases are categorized as surgically resectable². In addition, even after curative resection, most pancreatic cancers eventually recur, resulting in a 5-year survival rate for patients who have undergone curative resection of only 25%³. Long-term survival after curative resection can be influenced by several factors, including the presence of lymph node metastasis, tumor size, resection margin status, and histologic differentiation^{4–8}. However, although adjuvant chemotherapy, which might increase prolonged overall survival, could be considered after curative resection in patients with pathologic risk factors^{1,9}, quantitative imaging biomarkers based on preoperative imaging and their associations with clinical outcomes for pancreas head cancer have been rarely documented.

Morphologic heterogeneity is a pathologic finding that is used to characterize a malignant tumor; tumoral heterogeneity indicates the heterogeneous tumor cell population, differentiation, growth pattern, and desmoplastic stroma¹⁰. The biologic importance of intratumoral heterogeneity in malignant tumors has received attention in recent studies, and there is accumulating evidence that intratumoral heterogeneity at the cellular, molecular, and morphological levels has an important effect on tumor recurrence, therapeutic response, and survival in patients with malignant tumors, including pancreatic cancer^{10–12}. From the imaging perspective, intratumoral heterogeneity can be quantified non-invasively by computed tomography (CT) texture analysis, which has a potential role for predicting tumor types, treatment response, and prognosis in various cancers, including head and neck, esophageal, lung, breast, and colorectal cancers^{10,13–20}. Given the usefulness of CT texture analysis for prognosis predictions in various cancers, we have hypothesized that the quantitative texture features of pancreas head

¹Seoul National University Bundang Hospital, Department of Radiology, Seongnam, 13620, Korea. ²Hankuk University of Foreign Studies, Division of Biomedical Engineering, Yongin, 17035, Korea. ³Seoul National University Bundang Hospital, Department of Internal Medicine, Seongnam, 13620, Korea. Correspondence and requests for materials should be addressed to Y.H.K. (email: yhkrad@gmail.com)

Characteristic	Recurrence group (n = 70)	Non-recurrence group (n = 18)	P value
Sex			1.000
Male	37	9	
Female	33	9	
Mean age (year)	65.59 ± 10.23	60.44 ± 8.41	0.053
Tumor size			0.574
<2.5 cm	19	6	
≥2.5 cm	51	12	
Lymph node metastasis			0.038
Negative	27	12	
Positive	43	6	
Differentiation			1.000
well or moderately	64	17	
poorly	6	1	
Resection state			0.446
R0	59	17	
R1	11	1	

Table 1. Baseline Patient Characteristics.

cancer measured on preoperative CT images might be useful for predicting the clinical outcome of patients with pancreas head cancer after curative resection.

Therefore, the purpose of our study was to evaluate the association of survival outcomes with texture features on preoperative CT images by performing a texture analysis based on a histogram and grey level co-occurrence matrix (GLCM) in patients with pancreas head cancer who have undergone curative resection.

Results

Correlation of recurrence with clinical and pathologic features. The clinical and pathologic characteristics of the two groups are listed in Table 1. Out of 88 patients, there were 70 recurrences (79.5%) during the follow-up period. Among the clinical and pathologic variables, only the presence of lymph node metastasis was statistically different between the two groups (43 of 70 [61.4%] vs. 6 of 18 [33.3%], $P = 0.04$). For all the patients, the mean follow-up period was 26.3 months (range, 3.1–89 months) and the mean DFS (disease free survival) was 18 months (range, 0.3–89 months).

Correlation of recurrence with texture features. Regarding the CT texture features without filtration and with the various filter values, the areas under the curve (AUCs) and the optimal cut-off values for diagnosing recurrence determined by ROC curve analysis are summarized in Table 2. Without filtration and with fine (1.0) and medium (1.5 and 2) filter values, the recurrence group showed significantly lower averages, contrast and standard deviations, and higher correlations than the non-recurrence group. Only the average and contrast were significantly different between the two groups with the coarse filter (2.5) value. Applying cross-validation using Leave-one-out cross validation (LOOCV) model yielded the optimal cut-off values in concordance with the previous results (Supplementary Table S1).

Survival analysis: univariate and multivariate analysis. The results of the univariate Kaplan-Meier analysis and the multivariate Cox proportional hazards model are summarized in Tables 3 and 4, respectively. The univariate Kaplan-Meier analysis with the log-rank test for DFS showed significant differences for the presence of lymph node metastasis, the dichotomized average, contrast, correlation, and standard deviation with no filter and fine to medium filters and for the dichotomized average with the coarse filter (Table 3, Fig. 1). The cross-validation of Kaplan-Meier analysis by LOOCV model for DFS results were in line with the previous results (Table 3, Fig. 2). It showed statistically significant difference for most of the features except for correlation in the filter value of 0, average in the filter value of 1, standard deviation in the filter value of 1.5.

In the multivariate Cox proportional hazards model, the presence of lymph node metastasis was an independent factor that showed a significant association with DFS regardless of the applied filter (hazard ratio [HR], 1.957 to 2.181). Various texture features—including average filter values of 0, 1, and 2.5; standard deviation in the filter values of 0 and 2; contrast in the 1.5 filter value; and correlation in the filter value of 1—served as independent prognostic factors for predicting poorer DFS (Table 4). Overall, homogeneous texture features (lower standard deviation and contrast and higher correlation) with a lower average value from the texture analyses were significantly associated with poorer DFS.

Discussion

In this study, we have demonstrated the prognostic value of texture features of preoperative CT images using histograms and GLCM analyses in patients with pancreatic head cancer who have undergone curative resection. Our results show that lower average values with homogeneous features (lower standard deviation and contrast and

	Recurred group (n = 70)	Non-recurred group (n = 18)	P value	AUC	Cut-off value
Filter = 0					
ASM	0.001232	0.001312	0.9505		
Average	1088.4273	1102.1271	0.0021	0.736	≤1098.343478
Standard deviation	16.0277	17.4757	0.0065	0.709	≤16.194633
Kurtosis	0.02222	0.07221	0.6639		
Skewness	0.002466	0.1298	0.3157		
Contrast	192.5875	260.6758	0.00123	0.692	≤204.393377
Correlation	0.00241	0.001702	0.01	0.698	>0.002776
Entropy	6.8646	6.7437	0.7328		
Filter = 1					
ASM	0.0009825	0.0009885	0.6195		
Average	1084.1605	1101.4913	0.0021	0.736	≤1084.931174
Standard deviation	28.0968	30.9342	0.0094	0.699	≤31.434868
Kurtosis	-0.03283	-0.02773	0.5416		
Skewness	-0.04591	0.1201	0.0769		
Contrast	613.7428	856.2486	0.0199	0.679	≤905.806122
Correlation	0.000793	0.000548	0.0127	0.691	>0.000517
Entropy	7.0187	6.9823	0.5835		
Filter = 1.5					
ASM	0.001459	0.001371	0.9464		
Average	1084.307	1101.2969	0.0022	0.735	≤1088.576271
Standard deviation	15.3738	17.2526	0.0151	0.687	≤13.505866
Kurtosis	-0.04924	0.2372	0.1996		
Skewness	0.008841	0.08913	0.4079		
Contrast	111.4899	129.7122	0.0173	0.683	≤89.964225
Correlation	0.003265	0.002783	0.0169	0.683	>0.00398
Entropy	6.6663	6.7282	0.9094		
Filter = 2					
ASM	0.002261	0.002261	0.7999		
Average	1084.9351	1101.203	0.0024	0.733	≤1091.06089
Standard deviation	10.7231	12.3279	0.0314	0.665	≤10.579722
Kurtosis	-0.05305	0.157	0.1689		
Skewness	0.1835	0.1445	0.828		
Contrast	40.7814	46.7342	0.0159	0.685	≤34.290079
Correlation	0.007263	0.005749	0.0386	0.659	>0.008031
Entropy	6.28	6.3254	0.9176		
Filter = 2.5					
ASM	0.002952	0.002879	0.8604		
Average	1085.3756	1101.0749	0.0026	0.731	≤1092.655696
Standard deviation	9.2723	9.7441	0.0769		
Kurtosis	-0.1724	0.2028	0.0859		
Skewness	0.2459	0.1427	0.5835		
Contrast	26.9643	30.6362	0.0314	0.665	≤29.17734
Correlation	0.01012	0.009281	0.0769		
Entropy	6.0562	6.0853	0.9917		

Table 2. Medial Values of Measured Parameters, AUC and Cut-Off Values on ROC Analyses. *Note:* ASM = angular second moment; AUC = area under the curve.

higher correlation), along with the presence of lymph node metastasis, are significantly associated with poorer DFS, although the *P* values and HRs varied according to the applied filters.

In our study population, lower average values (without filtration and with filters 1.0 and 2.5) of pancreatic head cancer were found to be negative prognostic factors for DFS after curative resection in a multivariate Cox proportional hazards model. As the pixel histogram average represents the brightness or mean gray-level intensity of a region, a lower average on the texture analysis indicated a lesion with low attenuation. One of characteristic pathologic features of pancreas cancer is the presence of intense fibrosis in the tumor, which is known as desmoplastic reaction²¹. Previous studies have demonstrated that scirrhous carcinomas with abundant fibrosis and relative sparse tumor cells in the stomach, bile duct, breast, and colon have a poor prognosis^{22–25}. Now the

	Mean (month)	95% CI for the mean survival	P value	*LOOCV P value
Nodal status				
pN-	34.259	22.943 to 45.576	0.0013	
pN+	12.959	8.247 to 17.671		
Filter = 0				
Average \leq 1098.3434781	15.913	9.972 to 21.855	0.002	0.004
Average $>$ 1098.3434781	39.21	25.746 to 52.674		
Contrast \leq 204.3933771	14.815	8.456 to 21.173	0.0026	0.026
Contrast $>$ 204.3933771	33.434	22.208 to 44.659		
Correlation $>$ 0.002776	13.174	6.723 to 19.624	0.0131	0.12
Correlation \leq 0.002776	29.473	20.359 to 38.587		
Standard deviation \leq 16.194633	11.877	6.719 to 17.034	0.0006	0.002
Standard deviation $>$ 16.194633	33.051	22.839 to 43.262		
Filter = 1				
Average \leq 1084.931174	12.587	7.567 to 17.607	0.0035	0.582
Average $>$ 1084.931174	32.016	21.881 to 42.152		
Contrast \leq 905.806122	19.058	12.571 to 25.544	0.0083	0.019
Contrast $>$ 905.806122	27.328	18.624 to 36.032		
Correlation $>$ 0.000517	18.89	12.490 to 25.289	0.0056	0.012
Correlation \leq 0.000517	28.313	19.390 to 37.235		
Standard deviation std \leq 31.434868	19.003	12.633 to 25.373	0.0169	0.042
Standard deviation std $>$ 31.434868	33.911	20.819 to 47.003		
Filter = 1.5				
Average \leq 1088.576271	14.087	8.867 to 19.307	0.0061	0.056
Average $>$ 1088.576271	33.331	22.254 to 44.407		
Contrast \leq 89.964225	9.113	5.053 to 13.174	0.0003	0.001
Contrast $>$ 89.964225	29.913	21.190 to 38.637		
Correlation $>$ 0.00398	9.297	4.777 to 13.817	0.0013	0.258
Correlation \leq 0.00398	28.51	20.212 to 36.808		
Standard deviation \leq 13.505866	10.281	5.716 to 14.846	0.0081	0.416
Standard deviation $>$ 13.505866	28.288	19.944 to 36.633		
Filter = 2				
Average \leq 1091.06089	16.711	10.231 to 23.192	0.0102	0.046
Average $>$ 1091.06089	34.953	22.765 to 47.142		
Contrast \leq 34.290079	9.909	5.473 to 14.345	0.004	0.062
Contrast $>$ 34.290079	28.685	20.252 to 37.118		
Correlation $>$ 0.008031	13.208	7.956 to 18.461	0.0166	0.049
Correlation \leq 0.008031	29.884	20.293 to 39.475		
Standard deviation \leq 10.579722	12.884	8.028 to 17.740	0.0085	0.009
Standard deviation $>$ 10.579722	31.134	21.078 to 41.190		
Filter = 2.5				
Average \leq 1092.655696	16.533	10.171 to 22.896	0.0075	0.042
Average $>$ 1092.655696	35.692	23.260 to 48.124		

Table 3. Kaplan-Meier Survival Analysis for Disease-Free Survival According to Nodal Metastasis and Filter Levels. *Note:* *LOOCV (Leave-one-out cross validation).

evidence is accumulating that the fibrous component of a tumor correlates with its malignant behavior and contribute to therapeutic resistance²⁶. Although the significance of the fibrotic component of pancreas cancer is still unclear, peritumoral fibroblasts in pancreatic cancer have been shown to overexpress SPARC (secreted protein acidic and rich in cysteine), which is a marker of poor prognosis when expressed in the stroma²⁷. Furthermore, a desmoplastic reaction in pancreas cancer is thought to be responsible for metastasis, as well as chemotherapy resistance, by reducing the amount of drug delivered to the tumor²⁸. Because pancreatic cancer frequently has an abundant fibrotic stroma, which is seen as a hypo-attenuating mass in the early arterial phase with progressive delayed enhancement^{29,30}, we believe that the lower average observed on the pancreas phase images reflects pancreatic cancer with abundant desmoplastic reactions. Other studies have suggested that iso-attenuating pancreatic cancers on early-phase images tend to display less desmoplastic change within the mass and show better survival outcome^{25,31–36}. Studies involving diffusion MRI have concluded that the degree of fibrosis in pancreatic cancer cases correlates with diffusion restrictions related to poor prognosis^{37,38} and that it could be used to monitor treatment response³⁹. We speculate that pancreatic head cancer with a lower average may reflect an imaging phenotype

	HR	95% CI of HR	P value
Filter = 0			
Nodal metastasis	2.0375	1.2441 to 3.3378	0.0047
Average	0.5599	0.3201 to 0.9791	0.042
Standard deviation	0.5745	0.3467 to 0.9521	0.0315
Filter = 1			
Nodal metastasis	2.1257	1.2988 to 3.4793	0.0027
Average	0.5532	0.3254 to 0.9406	0.0288
Correlation	1.9806	1.0785 to 3.6364	0.0275
Filter = 1.5			
Nodal metastasis	1.957	1.1917 to 3.2137	0.008
Contrast	0.4665	0.2822 to 0.7712	0.003
Filter = 2			
Nodal metastasis	2.1457	1.3117 to 3.5099	0.0024
Standard deviation	0.5540	0.3459 to 0.8874	0.014
Filter = 2.5			
Nodal metastasis	2.1814	1.3344 to 3.5660	0.0019
Average	0.5190	0.3161 to 0.8521	0.0095

Table 4. Multivariate Cox Survival Analysis of Variables for Disease-Free Survival. *Note:* HR = hazard ratio.

of pancreatic cancer with abundant desmoplastic reactions that represents an aggressive subset of this cancer and that it might be related to poorer survival outcomes.

Our results are in line with the findings of Cassinotto *et al.*⁴⁰, who demonstrated that hypo-attenuating pancreatic cancer in the portal-venous phase on CT scans showed shorter DFS. However, the contrast between normal parenchyma and pancreatic cancer is greater in the pancreatic phase than in the portal-venous phase, and tumors normally demonstrate peripheral enhancement of the tumor in the portal-venous phase^{41–43}. Therefore, our data obtained from the pancreatic phase would be better for representing the entire tumor mass as well as the internal heterogeneity compared to the data from the portal-venous phase.

Also, interestingly, our study has revealed that both first- (a lower standard deviation without filtration and with the 2.0 filter) and second-order statistics (a lower contrast with the 1.5 filter and a higher correlation with the 1 filter) representing intratumoral homogeneity are related to poorer DFS in the multivariate Cox proportional hazards model. The first-order statistics, calculated from a histogram of pixel values, were based on the gray-level frequency distribution and represent a single pixel value rather than its spatial relation to adjacent pixels^{13,44}. Instead, secondary parameters, calculated using GLCM, show the spatial relationship between one pixel and another. These secondary parameters have the advantage of being able to quantify the overall texture content^{13,45}. Our study differs from the work of Cassinotto *et al.*⁴⁰, who only used first-order statistics to perform a texture analysis in pancreatic cancer, in that our results that were obtained using both first-order and second-order texture measures to better quantify heterogeneity within the pancreatic tumors. Our results suggest that homogenous features are correlated with poorer survival outcomes, in contrast to the majority of previous studies that found that increased tumoral heterogeneity on CT images is related to poorer clinical outcomes^{17,46–48}. Heterogeneity is a well-recognized feature of malignant tumors and presumably reflects alterations in the tissue microenvironment due to cell infiltration, angiogenesis, necrosis, and myxoid changes^{13,48,49}. In prior studies, tumor heterogeneity measured on CT images correlated with histologic findings of an irregular, disorganized architectural distortion from angiogenesis and hypoxia in primary colorectal cancer and non-small-cell lung cancer^{50,51}. However, contradictory findings were found in studies of primary¹⁵ and metastatic colorectal cancer⁵², where texture variables representing less heterogeneity (e.g., lower entropy and standard deviations) were associated with poorer survival. Based on our study results, as well as those of the studies mentioned above (15, 53), we conjecture that homogeneous texture features could represent more aggressive behavior in tumors, thereby representing higher cellular density or dense desmoplasia. Our study results therefore imply that texture analysis on pre-operative CT scans may be potentially used to identify patients who have a higher chance of recurrence after curative resection and therefore would benefit from extensive postoperative surveillance and adjuvant therapy. Moreover, multiple ongoing studies are focused on validating the benefit of neoadjuvant chemotherapy in patients with resectable or borderline resectable pancreatic cancer, although there are no data that clearly suggest improved survival with neoadjuvant chemotherapy⁵³. In addition to endoscopic ultrasound or measuring serum

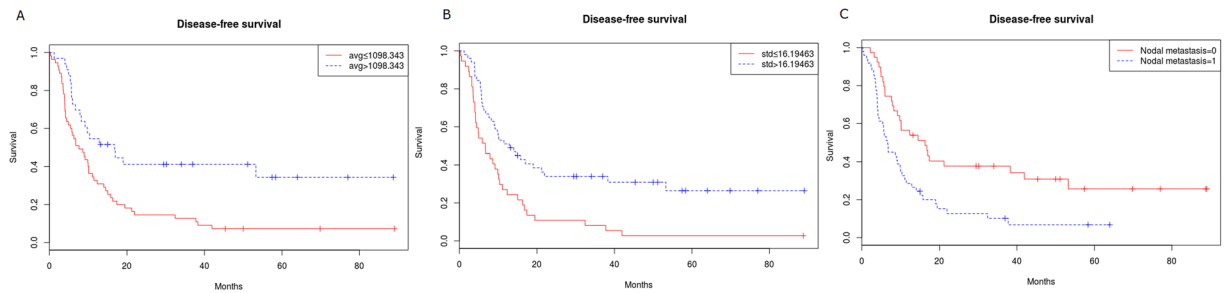


Figure 1. Kaplan-Meier survival curves without filtration show significant difference in disease free survival rates according to stratified (A) Average, (B) Standard deviation, (C) Nodal metastasis with log-rank P values of 0.002, 0.0006 and 0.013, respectively.

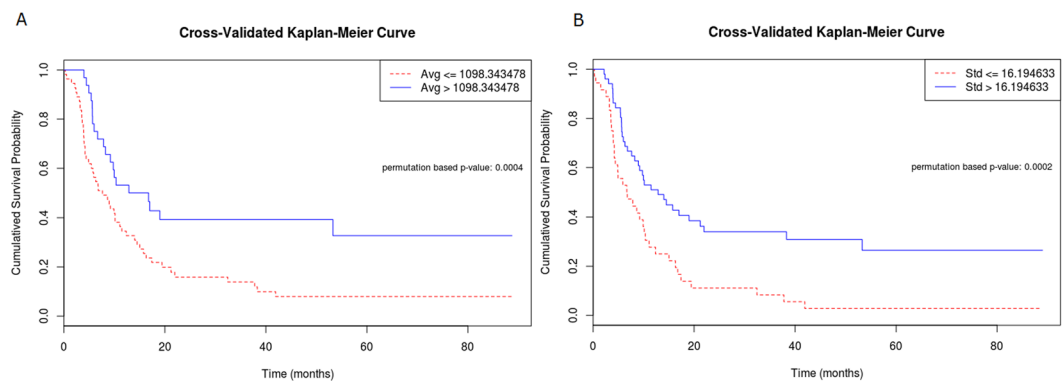


Figure 2. Cross-validated Kaplan-Meier survival curves without filtration show significant difference in disease free survival rates according to stratified (A) Average, (B) Standard deviation with log-rank P values of 0.0004, 0.0002, respectively.

CA 19-9 levels for the selection of candidates for neoadjuvant therapy^{54–56}, the ability to stratify prognosis in patients with initially resectable pancreas head cancer by performing texture analyses of routine preoperative CT images could be helpful for selecting candidates for neoadjuvant chemotherapy. Further research is warranted to confirm the correlation between texture features and clinical outcomes in a prospective, larger cohort and to determine whether the prognostic information from texture analyses could be clinically utilized for patients with pancreatic head cancer.

Several limitations need to be addressed with respect to our study. First, as this study was retrospectively designed, the possibility of selection bias should be considered. Second, we did not take into account potential variables affecting tumor enhancement on the contrast-enhanced CT scans, including cardiac output, body mass, and blood volume. Third, although the texture parameters are relatively insensitive to the CT acquisition factors⁵⁷, the use of three different types of scanners in our study might have resulted in the inherent variability of the texture features. Future studies using the same scanner and CT acquisition protocol to reduce other possible factors affecting texture analysis are required. Fourth, given that the external validation was not performed in our study, we cannot be certain that the result in our study could be applied to the external, prospectively recruited patients. Nonetheless, the LOOCV used for cross-validation was shown to strengthen the reliability of our study results. Thus, while the results of our study cannot be immediately applied to clinical practice, further prospective validation studies using large multicentre datasets are warranted. Lastly, contrary to several reports suggesting that 3-dimensional (3D) analysis would better account for tumor heterogeneity⁵⁸, we performed a 2-dimensional (2D) quantitative tumor analysis by selecting the single axial image with largest tumor area. In addition, aside from the fact that 3D whole-tumor analysis is complex and time-consuming, recent studies have shown that there is no difference between 2D and 3D tumor analyses⁵².

Despite several limitations in our study, it is the first to investigate the association of first and second texture features with the prognosis in pancreas cancer head patients. In the era of Radiomics, the need for standardization is increasing to provide clinically relevant results. The number of patients included in our study was within the suggested value (10–15 patients per feature) to test prognostic power of texture features. Furthermore, we have provided details of methods used in the analysis and included clinically important variables in the analysis. Our study provides that texture-feature-based image analysis holds promise in predicting prognosis in pancreas head cancer patients, and that the prospective clinical studies may be needed to better delineate the potential of this approach.

In conclusion, lower average and standard deviation values from CT texture analyses are associated with poorer survival outcomes in pancreas head cancer patients who underwent curative resection. Texture analysis

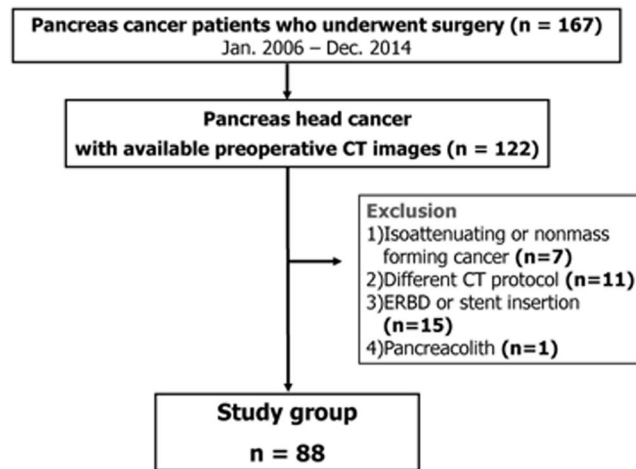


Figure 3. Flow chart showing patient selection criteria of our study.

features from routinely performed pre-operative CT images could be used as an independent imaging parameter for predicting the prognosis in these patients.

Materials and Methods

Seoul National University Bundang Hospital institutional review board approval was obtained for this study, and informed consent was waived. All methods were performed in accordance with the relevant guidelines and regulations.

Patients. From January 2006 to December 2014, 167 patients underwent resection for pancreas cancer in our institution. Among them, 122 patients who had a histopathologic diagnosis of ductal adenocarcinoma in the pancreas head were initially included in this study. Of these 122 patients, 27 patients were excluded from this study for the following reasons, as these factors could potentially influence the texture values: biliary stent placement along the common duct prior to CT examination ($n = 15$), different CT protocols ($n = 11$), and pancreatolith in the pancreas head area ($n = 1$). Additionally, 7 patients were excluded because their pancreas head cancers were not identifiable on the initial CT images. Finally, 88 patients were included as the sample group for our study (Fig. 3). None of these included 88 patients had undergone either preoperative radiation or chemotherapy.

CT imaging protocol. All patients underwent preoperative contrast-enhanced CT imaging with a pancreas protocol. After the acquisition of non-contrast images, iopromide, an intravenous contrast material (Ultravist 370; Bayer, Berlin, Germany) was injected via the antecubital vein using a power injector (Stellant D; Medrad, Indianola, PA) at a dose of 2 mL per kilogram of body weight at a rate of 3 mL/sec. CT scans of the pancreatic and portal venous phase were initiated after the bolus contrast media injection with delays of 20 and 60 seconds after aortic enhancement of 150 HU, respectively. Non-contrast and pancreatic phase images were acquired from the diaphragm to the umbilicus level, and portal venous phase images were obtained from the diaphragm to symphysis pubis level. Images were acquired with 16- ($n = 35$), 64- ($n = 39$), or 128- ($n = 14$) multi-detector CT scanners (Mx 8000, Brilliance 64, iCT256; Philips Medical Systems, Cleveland, OH). The scanning parameters were as follows: 16×1.5 , 64×0.625 , or 128×0.625 mm collimation; a rotation speed of 0.5 s; a pitch of 1.25, 0.641, or 0.993; a kVp of 120. Effective mAs ranged from 72 to 385 mAs using an automatic tube current modulation technique (Dose-Right; Philips Medical Systems). The CT images were reconstructed using filtered back projection with 4-mm thick sections at 3-mm increments.

Quantitative texture analysis. The pancreatic-phase CT images were retrieved from the picture archiving and communication system and transferred to an independent workstation for further texture analysis using software built in-house. After selecting the single axial pancreatic-phase CT image⁴¹ showing the largest cross-sectional area of the pancreas head cancer, a polygonal region of interest (ROI) was manually drawn as large as possible within the tumor border with the consensus of two radiologists (K.Y.H. and Y.G.B., with 20 and 3 years of experience in abdominal imaging, respectively) who were blinded to the pathologic and clinical outcomes (Fig. 4). Particular attention was paid to avoiding the peripancreatic vessels while delineating the ROIs for each case. Areas of air and fatty tissues were removed from the analyses by excluding any pixels with attenuation values less than 0 Hounsfield units. Although the contouring was performed on the pancreatic-phase CT images, the portal-venous-phase CT or magnetic resonance imaging (MRI) scans were also reviewed to check whether the ROIs were accurately drawn. The median tumor areas and the number of pixels in the ROIs for the texture analyses were 132.8 cm^2 (range, 61.3 to 597.6) and 433.3 (range, 164 to 1,685), respectively.

Laplacian of the Gaussian band-pass filter was applied to detect intensity changes within the images smoothed by Gaussian distribution based on the filter sigma value^{17,59}. This resulted in the images displaying features at different scales (from fine to coarse textures) associated with filter sigma values within the ROI around the pancreas head cancer. The scale was determined by filter sigma values of 1.0 (fine texture, filter width 4 pixels),

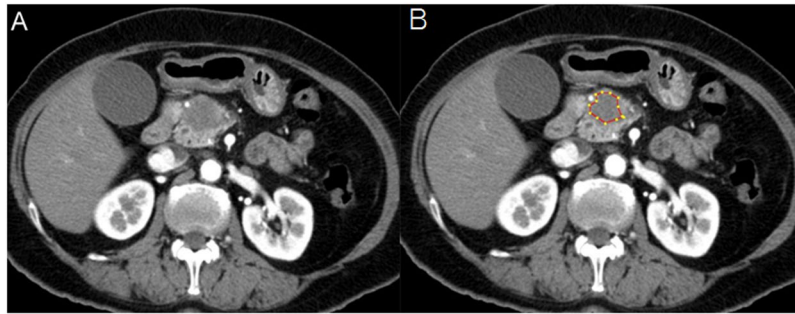


Figure 4. An example of quantitative texture analysis of the pancreas head cancer. (A) Axial pancreatic phase CT scan shows a low attenuating mass in the pancreas head. (B) ROI was drawn excluding fat or air densities for texture analysis.

1.5 to 2.0 (medium texture, filter width 6–10 pixels), and 2.5 (coarse texture, filter width 12 pixels)¹⁷. The degree of image smoothing was proportional to the filter value: a higher (or lower) filter value enabled the extraction of a coarse (or fine) texture by smoothing the images to a greater (or lesser) degree⁵⁹. The distributions of pixel values of the gray-level histograms within the ROIs were characterized by average (mean intensity of the gray-level distribution), standard deviation (the degree of dispersion), kurtosis (flatness of the histogram), and skewness (asymmetry of the histogram). Texture parameters, including angular second moment (or energy; uniformity in gray-level distribution), entropy (randomness of pixel distribution), correlation (measurement of gray-level linear dependence), and contrast (measurement of local variations) were calculated by GLCM, which represents the spatial dependence relationship between groups of neighboring pixel intensity values^{13,14,45}. In general, a higher standard deviation of the pixel distribution, a higher kurtosis, a positive or negative skewness, a higher entropy, and a higher contrast and lower angular second moment and correlation represented increased heterogeneity^{14–17,45}.

Review of pathologic and clinical follow-up data. The pathologic and clinical follow-up data were reviewed by one radiologist (Y.J.L., with 9 years of experience in abdominal imaging). The final histopathologic reports of the surgically excised specimens were also reviewed for tumor size, presence of lymph node metastasis, resection margin involvement, and pathologic differentiation according to the 7th American Joint Committee on Cancer staging system⁶⁰. The pathologic results were dichotomized as follows: smaller than 2.5 cm or larger than or equal to 2.5 cm for size, positive or negative for lymph node metastasis, positive (R1) or negative (R0) for surgical margins, and well to moderately or poorly differentiated pathologic differentiation⁶¹. After surgery, all patients underwent clinical follow-up according to our institutional protocol, including serum cancer antigen (CA) 19-9 measurement and CT examinations at 3- to 6-month intervals. Medical records and CT examinations following surgical resection were reviewed, focusing on the presence and date of tumor recurrence or death and last follow-up date. Tumor recurrence was determined by the presence of locoregional recurrence or distant metastasis documented on a patient's medical record based on physical examination, laboratory findings, follow-up imaging studies, and pathologic reports of biopsy samples, if available. Then the patients were classified into recurrence and non-recurrence groups. DFS was defined as the period from resection to the diagnosis of the tumor recurrence or to any cause of death. The final data were collected on March 31, 2017. Patients without recurrence on the date of the most recent follow-up were censored in the analysis.

Statistical analysis. The clinicopathologic results and CT texture features were compared between the recurrence and non-recurrence groups. The univariate analysis for categorical variables was performed using the chi-square test. A Mann-Whitney U test was performed to compare the continuous variables between the two groups. To dichotomize the texture features with or without filters for the survival analysis, the optimal cut-off values were determined by the value which maximizes the sum of sensitivity and specificity on a receiver-operating characteristic (ROC) curve analysis. To improve the power of prediction, additional cross-validation of the results using Leave-one-out cross validation (LOOCV) test was adopted. In LOOCV, multiple rounds of ROC analysis are carried out by using the training data and then the validation data are assigned to dichotomized group based on the cut-off point. The cut-off point selected most frequently was defined as optimized cut-off value in the LOOCV analysis. DFS was analyzed by using Kaplan-Meier method based on each of the cut-off values calculated by the ROC curve analysis, and comparisons of the dichotomized variables between groups were performed by a log-rank test. Additionally, LOOCV cross-validated Kaplan-Meier analysis was performed (Table 3). A multivariate Cox proportional hazards model with a hierarchical forward step-wise procedure was used to assess whether the texture features with or without filters were independently and significantly associated with DFS. Variables with *P* values less than 0.05 in the univariate Kaplan-Meier analysis were entered into a multivariate Cox proportional hazards model. All analyses were performed using SPSS version 14.0 (Chicago, IL) and Medcalc version 12.1.4.0 (Medcalc Software, Ostend, Belgium). *P* values less than 0.05 were considered to be statistically significant.

References

- Hidalgo, M. Pancreatic cancer. *New England Journal of Medicine* **362**, 1605–1617 (2010).
- Konstantinidis, I. T. *et al.* Pancreatic ductal adenocarcinoma: is there a survival difference for R1 resections versus locally advanced unresectable tumors? What is a “true” R0 resection? *Annals of surgery* **257**, 731–736 (2013).
- Kamisawa, T., Wood, L. D., Itoi, T. & Takaori, K. Pancreatic cancer. *The Lancet* **388**, 73–85 (2016).
- Winter, J. M. *et al.* 1423 pancreaticoduodenectomies for pancreatic cancer: a single-institution experience. *Journal of gastrointestinal surgery* **10**, 1199–1211 (2006).
- El Nakeeb, A. *et al.* Prognostic factors affecting survival after pancreaticoduodenectomy for pancreatic adenocarcinoma (single center experience). *Hepato-gastroenterology* **61**, 1426–1438 (2013).
- Wagner, M. *et al.* Curative resection is the single most important factor determining outcome in patients with pancreatic adenocarcinoma. *British Journal of Surgery* **91**, 586–594 (2004).
- Brennan, M. F., Kattan, M. W., Klimstra, D. & Conlon, K. Prognostic nomogram for patients undergoing resection for adenocarcinoma of the pancreas. *Annals of surgery* **240**, 293–298 (2004).
- Geer, R. J. & Brennan, M. F. Prognostic indicators for survival after resection of pancreatic adenocarcinoma. *The American journal of surgery* **165**, 68–73 (1993).
- Lim, J. E., Chien, M. W. & Earle, C. C. Prognostic factors following curative resection for pancreatic adenocarcinoma: a population-based, linked database analysis of 396 patients. *Annals of surgery* **237**, 74–85 (2003).
- Verbeke, C. Morphological heterogeneity in ductal adenocarcinoma of the pancreas - Does it matter? *Pancreatology: official journal of the International Association of Pancreatology (IAP) ... [et al.]* **16**, 295–301, <https://doi.org/10.1016/j.pan.2016.02.004> (2016).
- Meacham, C. E. & Morrison, S. J. Tumour heterogeneity and cancer cell plasticity. *Nature* **501**, 328–337 (2013).
- Bandyopadhyay, S. *et al.* Isolated solitary ducts (naked ducts) in adipose tissue: a specific but underappreciated finding of pancreatic adenocarcinoma and one of the potential reasons of understaging and high recurrence rate. *The American journal of surgical pathology* **33**, 425–429 (2009).
- Davnall, F. *et al.* Assessment of tumor heterogeneity: an emerging imaging tool for clinical practice? *Insights into imaging* **3**, 573–589, <https://doi.org/10.1007/s13244-012-0196-6> (2012).
- Ganeshan, B., Skogen, K., Pressney, I., Coutroubis, D. & Miles, K. Tumour heterogeneity in oesophageal cancer assessed by CT texture analysis: preliminary evidence of an association with tumour metabolism, stage, and survival. *Clinical radiology* **67**, 157–164, <https://doi.org/10.1016/j.crad.2011.08.012> (2012).
- Ng, F., Ganeshan, B., Kozarski, R., Miles, K. A. & Goh, V. Assessment of primary colorectal cancer heterogeneity by using whole-tumor texture analysis: contrast-enhanced CT texture as a biomarker of 5-year survival. *Radiology* **266**, 177–184, <https://doi.org/10.1148/radiol.12120254> (2013).
- Bashir, U., Siddique, M. M., McLean, E., Goh, V. & Cook, G. J. Imaging Heterogeneity in Lung Cancer: Techniques, Applications, and Challenges. *AJR. American journal of roentgenology* **207**, 534–543, <https://doi.org/10.2214/ajr.15.15864> (2016).
- Yip, C. *et al.* Primary esophageal cancer: heterogeneity as potential prognostic biomarker in patients treated with definitive chemotherapy and radiation therapy. *Radiology* **270**, 141–148, <https://doi.org/10.1148/radiol.13122869> (2014).
- Yoon, S. H. *et al.* Tumor Heterogeneity in Human Epidermal Growth Factor Receptor 2 (HER2)-Positive Advanced Gastric Cancer Assessed by CT Texture Analysis: Association with Survival after Trastuzumab Treatment. *PLoS one* **11**, e0161278, <https://doi.org/10.1371/journal.pone.0161278> (2016).
- Kim, J. H. *et al.* Breast Cancer Heterogeneity: MR Imaging Texture Analysis and Survival Outcomes. *Radiology* **282**, 665–675, <https://doi.org/10.1148/radiol.2016160261> (2017).
- Phillips, I. *et al.* Clinical applications of textural analysis in non-small cell lung cancer. *Br J Radiol* **91**, 20170267, <https://doi.org/10.1259/bjr.20170267> (2018).
- Erkan, M. *et al.* Cancer-stellate cell interactions perpetuate the hypoxia-fibrosis cycle in pancreatic ductal adenocarcinoma. *Neoplasia* **11**, 497–508 (2009).
- Aranha, G. V. & Georgen, R. Gastric linitis plastica is not a surgical disease. *Surgery* **106**, 758–762; discussion 762–753 (1989).
- Amorn, Y. & Knight, W. A. Primary linitis plastica of the colon. *Report of two cases and review of the literature. Cancer* **41**, 2420–2425 (1978).
- Dawson, P. J., Karrison, T. & Ferguson, D. J. Histologic features associated with long-term survival in breast cancer. *Human pathology* **17**, 1015–1021 (1986).
- Blouhos, K. *et al.* Surgically proved visually isoattenuating pancreatic adenocarcinoma undetected in both dynamic CT and MRI. Was blind pancreaticoduodenectomy justified? *International journal of surgery case reports* **4**, 466–469 (2013).
- Iwatsuki, M. *et al.* Epithelial–mesenchymal transition in cancer development and its clinical significance. *Cancer science* **101**, 293–299 (2010).
- Von Hoff, D. *et al.* Frequency of potential therapeutic targets identified by immunohistochemistry (IHC) and DNA microarray (DMA) in tumors from patients who have progressed on multiple therapeutic agents. *Journal of Clinical Oncology* **24**, 3071–3071 (2006).
- Li, X. *et al.* Targeting the cancer-stroma interaction: a potential approach for pancreatic cancer treatment. *Current pharmaceutical design* **18**, 2404–2415 (2012).
- Demachi, H. *et al.* Histological influence on contrast-enhanced CT of pancreatic ductal adenocarcinoma. *Journal of computer assisted tomography* **21**, 980–985 (1997).
- Ichikawa, T. [A comparative study of histopathological findings and CT images related to pancreatic carcinomas. An attempt at diagnosis in tissue characterization by CT]. *Nihon Ika Daigaku zasshi* **59**, 23–29 (1992).
- Itoh, S. *et al.* Pancreatic ductal adenocarcinoma showing iso-attenuation in early-phase contrast-enhanced CT: comparison with histopathological findings. *Radiation medicine* **20**, 59–67 (2001).
- Hattori, Y. *et al.* Enhancement patterns of pancreatic adenocarcinoma on conventional dynamic multi-detector row CT: correlation with angiogenesis and fibrosis. *World journal of gastroenterology* **15**, 3114–3121 (2009).
- Yoon, S. H. *et al.* Small (≤ 20 mm) pancreatic adenocarcinomas: analysis of enhancement patterns and secondary signs with multiphasic multidetector CT. *Radiology* **259**, 442–452 (2011).
- Takeshita, K. *et al.* Imaging of early pancreatic cancer on multidetector row helical computed tomography. *The British journal of radiology* (2014).
- Bluemke, D. A. *et al.* Potentially resectable pancreatic adenocarcinoma: spiral CT assessment with surgical and pathologic correlation. *Radiology* **197**, 381–385 (1995).
- Takeshita, K. *et al.* Imaging of early pancreatic cancer on multidetector row helical computed tomography. *The British journal of radiology* **83**, 823–830, <https://doi.org/10.1259/bjr/80905803> (2010).
- Muraoka, N. *et al.* Apparent diffusion coefficient in pancreatic cancer: characterization and histopathological correlations. *Journal of Magnetic Resonance Imaging* **27**, 1302–1308 (2008).
- Wang, Y. *et al.* Diffusion-weighted magnetic resonance imaging of pancreatic adenocarcinomas: Association with histopathology and tumor grade. *Journal of Magnetic Resonance Imaging* **33**, 136–142 (2011).
- Ma, W. *et al.* Apparent Diffusion Coefficient and Dynamic Contrast-Enhanced Magnetic Resonance Imaging in Pancreatic Cancer: Characteristics and Correlation With Histopathologic Parameters. *Journal of computer assisted tomography* **40**, 709–716 (2016).

40. Cassinotto, C. *et al.* Resectable pancreatic adenocarcinoma: Role of CT quantitative imaging biomarkers for predicting pathology and patient outcomes. *European journal of radiology* **90**, 152–158 (2017).
41. Fletcher, J. G. *et al.* Pancreatic malignancy: value of arterial, pancreatic, and hepatic phase imaging with multi-detector row CT. *Radiology* **229**, 81–90, <https://doi.org/10.1148/radiol.2291020582> (2003).
42. Lu, D. *et al.* Two-phase helical CT for pancreatic tumors: pancreatic versus hepatic phase enhancement of tumor, pancreas, and vascular structures. *Radiology* **199**, 697–701 (1996).
43. Boland, G. *et al.* Pancreatic-phase versus portal vein-phase helical CT of the pancreas: optimal temporal window for evaluation of pancreatic adenocarcinoma. *AJR. American journal of roentgenology* **172**, 605–608 (1999).
44. Amadasun, M. & King, R. Textural features corresponding to textural properties. *IEEE Transactions on systems, man, and Cybernetics* **19**, 1264–1274 (1989).
45. Rao, C. N., Sastry, S. S., Mallika, K., Tieng, H. S. & Mahalakshmi, K. Co-occurrence matrix and its statistical features as an approach for identification of phase transitions of mesogens. *Int. J. Innov. Res. Sci. Eng. Technol* **2**, 4531–4538 (2013).
46. Zhang, H. *et al.* Locally advanced squamous cell carcinoma of the head and neck: CT texture and histogram analysis allow independent prediction of overall survival in patients treated with induction chemotherapy. *Radiology* **269**, 801–809, <https://doi.org/10.1148/radiol.13130110> (2013).
47. Cui, C. *et al.* Quantitative analysis and prediction of regional lymph node status in rectal cancer based on computed tomography imaging. *European radiology* **21**, 2318–2325 (2011).
48. Ganeshan, B., Panayiotou, E., Burnand, K., Dizdarevic, S. & Miles, K. Tumour heterogeneity in non-small cell lung carcinoma assessed by CT texture analysis: a potential marker of survival. *European radiology* **22**, 796–802 (2012).
49. Lunt, S. J., Chaudary, N. & Hill, R. P. The tumor microenvironment and metastatic disease. *Clinical & experimental metastasis* **26**, 19–34 (2009).
50. Ganeshan, B. *et al.* Non-small cell lung cancer: histopathologic correlates for texture parameters at CT. *Radiology* **266**, 326–336 (2013).
51. Ganeshan, B. & Miles, K. A. Quantifying tumour heterogeneity with CT. *Cancer Imaging* **13**, 140 (2013).
52. Lubner, M. G. *et al.* CT textural analysis of hepatic metastatic colorectal cancer: pre-treatment tumor heterogeneity correlates with pathology and clinical outcomes. *Abdominal imaging* **40**, 2331–2337 (2015).
53. Wong, J., Solomon, N. L. & Hsueh, C.-T. Neoadjuvant treatment for resectable pancreatic adenocarcinoma. *World journal of clinical oncology* **7**, 1 (2016).
54. Yovino, S., Darwin, P., Daly, B., Garofalo, M. & Moesinger, R. Predicting unresectability in pancreatic cancer patients: the additive effects of CT and endoscopic ultrasound. *Journal of gastrointestinal surgery: official journal of the Society for Surgery of the Alimentary Tract* **11**, 36–42, <https://doi.org/10.1007/s11605-007-0110-6> (2007).
55. Bergquist, J. R. *et al.* Carbohydrate Antigen 19-9 Elevation in Anatomically Resectable, Early Stage Pancreatic Cancer Is Independently Associated with Decreased Overall Survival and an Indication for Neoadjuvant Therapy: A National Cancer Database Study. *Journal of the American College of Surgeons* **223**, 52–65, <https://doi.org/10.1016/j.jamcollsurg.2016.02.009> (2016).
56. Katz, M. H. *et al.* Serum CA 19-9 as a marker of resectability and survival in patients with potentially resectable pancreatic cancer treated with neoadjuvant chemoradiation. *Annals of surgical oncology* **17**, 1794–1801, <https://doi.org/10.1245/s10434-010-0943-1> (2010).
57. Miles, K. A., Ganeshan, B., Griffiths, M. R., Young, R. C. & Chatwin, C. R. Colorectal cancer: texture analysis of portal phase hepatic CT images as a potential marker of survival. *Radiology* **250**, 444–452, <https://doi.org/10.1148/radiol.2502071879> (2009).
58. Ng, F., Kozarski, R., Ganeshan, B. & Goh, V. Assessment of tumor heterogeneity by CT texture analysis: can the largest cross-sectional area be used as an alternative to whole tumor analysis? *European journal of radiology* **82**, 342–348 (2013).
59. Ganeshan, B., Miles, K. A., Young, R. C. & Chatwin, C. R. Texture analysis in non-contrast enhanced CT: impact of malignancy on texture in apparently disease-free areas of the liver. *European journal of radiology* **70**, 101–110, <https://doi.org/10.1016/j.ejrad.2007.12.005> (2009).
60. Compton, C. C. *et al.* *AJCC cancer staging atlas: a companion to the seventh editions of the AJCC cancer staging manual and handbook.* (Springer Science & Business Media, 2012).
61. Chang, S. T. *et al.* Preoperative Multidetector CT Diagnosis of Extrapancreatic Perineural or Duodenal Invasion Is Associated with Reduced Postoperative Survival after Pancreaticoduodenectomy for Pancreatic Adenocarcinoma: Preliminary Experience and Implications for Patient Care. *Radiology* **281**, 816–825, <https://doi.org/10.1148/radiol.2016152790> (2016).

Author Contributions

Y.K., G.Y. designed the study. and G.Y. wrote the majority of the manuscript. D.C., Y.K., G.Y. analyzed and interpreted the data. B.K., D.C. contributed image analysis tool. Y.L., G.Y. prepared the pathologic, follow up database, tables and figures. Y.K., B.K., J.H. indexed relevant references, supervised and edited the paper. All authors reviewed the manuscript.

Additional Information

Supplementary information accompanies this paper at <https://doi.org/10.1038/s41598-018-25627-x>.

Competing Interests: The authors declare no competing interests.

Publisher's note: Springer Nature remains neutral with regard to jurisdictional claims in published maps and institutional affiliations.



Open Access This article is licensed under a Creative Commons Attribution 4.0 International License, which permits use, sharing, adaptation, distribution and reproduction in any medium or format, as long as you give appropriate credit to the original author(s) and the source, provide a link to the Creative Commons license, and indicate if changes were made. The images or other third party material in this article are included in the article's Creative Commons license, unless indicated otherwise in a credit line to the material. If material is not included in the article's Creative Commons license and your intended use is not permitted by statutory regulation or exceeds the permitted use, you will need to obtain permission directly from the copyright holder. To view a copy of this license, visit <http://creativecommons.org/licenses/by/4.0/>.

© The Author(s) 2018